

# Interfacial Composition and Microstructure of $\text{Fe}_3\text{O}_4$ Magnetic Tunnel Junctions

Chando Park, Yiming Shi, Yingguo Peng, Katayun Barmak, Jian-Gang Zhu, David E. Laughlin, and Robert M. White

**Abstract**—Magnetic tunnel junctions with an  $\text{Fe}_3\text{O}_4$  top electrode have been fabricated. High resolution transmission electron microscopy (HRTEM) shows that in as-deposited state, Fe and FeO phases exist at the interface. These two phases are believed to have formed as a result of the unstable plasma condition at the start of the  $\text{Fe}_3\text{O}_4$  deposition. A relatively low magnetoresistance ratio (MR) (3.5%) and low switching field ( $H_{C2}$ ) (40 Oe) is observed which is associated with the fact that the FeO phase magnetically isolates the Fe phase from the  $\text{Fe}_3\text{O}_4$  phase at the interface. After annealing at 150 °C for 5 h, the MR as well as the switching field ( $H_{C2}$ ) increases by a factor of two. HRTEM shows that the FeO phase at the interface has transformed into Fe and  $\text{Fe}_3\text{O}_4$  in the annealed sample, resulting in the increased MR (7.0%) and higher switching field ( $H_{C2}$ ) (300 Oe). However, annealing does not completely remove Fe at the interface, thereby limiting the MR.

**Index Terms**—Half-metallic, magnetic tunnel junction, magnetite, magnetoresistance ratio.

## I. INTRODUCTION

AS A RESULT of their high spin polarization (100%), half-metallic materials having only one spin-subband at the Fermi level are very attractive as electrodes in magnetic tunnel junctions (MTJ) [1]. Several materials such as Heusler alloys (NiMnSb), chromium dioxide ( $\text{CrO}_2$ ), Perovskites ( $\text{La}_{0.7}\text{Sr}_{0.3}\text{MnO}_3$ ), and magnetite ( $\text{Fe}_3\text{O}_4$ ) are expected to be half-metallic [2]–[4]. Among these,  $\text{Fe}_3\text{O}_4$  has the highest Curie temperature (858 K) and is therefore considered to be the most promising choice for tunneling magnetoresistive devices [4]. However, recent studies show that the observed MR ratio is much lower than expected when  $\text{Fe}_3\text{O}_4$  is used as an electrode [5]–[7], and, in fact, in some cases an MTJ fails to form [8]. To date, at least three reasons for the low observed MR have been suggested: 1) a disordered spin structure at the interface of  $\text{Fe}_3\text{O}_4$  that reduces the spin polarization [5]; 2) some reduction of  $\text{Fe}_3\text{O}_4$  due to the Al may introduce other phases such as Fe and FeO, resulting in a reduced MR [4], [5]; and 3) a magnetic dead layer at the interface of the  $\text{Fe}_3\text{O}_4$  [9]. It should be noted that all three of these effects are associated with the interface.

In this study, the structure and magnetic properties of  $\text{Fe}_3\text{O}_4$  films deposited via reactive sputtering are investigated. In particular, the  $\text{AlO}_x/\text{Fe}_3\text{O}_4$  interface is examined using high resolution transmission electron microscopy (HRTEM), and the pres-

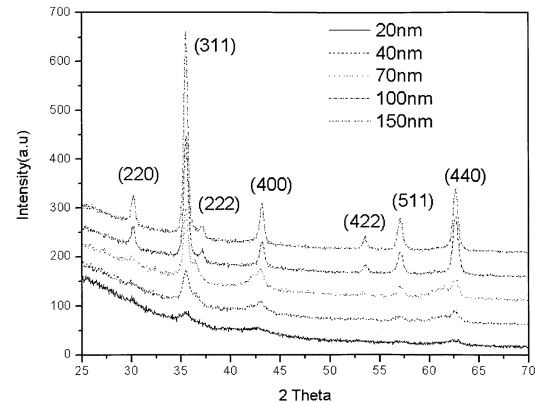


Fig. 1. Glancing-angle XRD patterns of  $\text{Fe}_3\text{O}_4$  films with different thicknesses.

ence of interfacial Fe and FeO is related to the magnetic and magnetoresistive behavior of the junctions.

## II. EXPERIMENTAL PROCEDURES

Single-layer thin films of  $\text{Fe}_3\text{O}_4$ , with thicknesses in the range of 20–150 nm, and layered stacks of Ta 5 nm/NiFe 10 nm/ $\text{AlO}_x$  2.5 nm/ $\text{Fe}_3\text{O}_4$  30 nm/Ta 5 nm, with  $\text{Fe}_3\text{O}_4$  as the top layer, were deposited on oxidized silicon substrates. The substrates were ultrasonically cleaned in acetone and alcohol for 15 min and rinsed in deionized (DI) water. The base pressure was  $3 \times 10^{-7}$  torr. The deposition pressure and temperature were 5 mT and room temperature, respectively. The thin barrier layer of  $\text{AlO}_x$  was formed by plasma oxidation of 2.5 nm of metallic Al for 70 s, prior to the deposition of the top magnetite electrode. The magnetite layer was fabricated by reactive sputtering of Fe in flowing oxygen. Oxygen and argon gases were introduced through the top of the chamber and their flow rates were 6.8 sccm and 27 sccm, respectively. The patterning of the junctions was accomplished through the use of a shadow mask during deposition. The phase identity and microstructure of the films were investigated by HRTEM and X-ray diffraction (XRD). For the XRD studies, the incoming beam was incident at a glancing angle of  $0.5^\circ$ . The magnetic properties of the samples were measured using an alternating gradient magnetometer (AGM) in fields up to 2 kOe. The transfer curves of the junctions were measured by a four-point measurement in fields up to 1000 Oe.

## III. RESULTS AND DISCUSSION

The glancing-angle XRD patterns for single-layer  $\text{Fe}_3\text{O}_4$  films of different thicknesses are presented in Fig. 1. All the

Manuscript received January 6, 2003. This work was supported by the Pittsburgh Digital Greenhouse and the Data Storage Systems Center at Carnegie Mellon University.

The authors are with the Data Storage Systems Center, Carnegie Mellon University, Pittsburgh, PA 15213 USA (e-mail: chando@Andrew.cmu.edu).

Digital Object Identifier 10.1109/TMAG.2003.815718

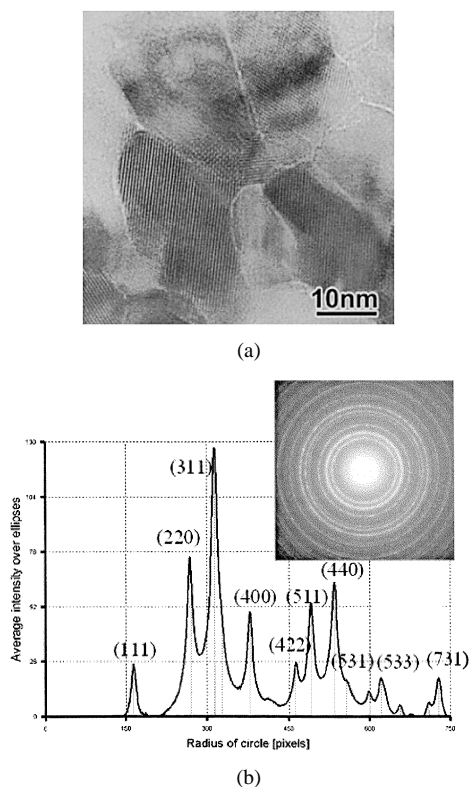


Fig. 2. (a) Plan view transmission electron micrograph, and (b) selected area diffraction pattern (SADP) and the intensity profile along the radius direction [10] for a 100-nm-thick Fe<sub>3</sub>O<sub>4</sub> film.

peaks can be assigned to magnetite. The figure further shows that Fe<sub>3</sub>O<sub>4</sub> can be formed in films as thin as 20 nm. The TEM image in Fig. 2(a) demonstrates that the iron oxide film is polycrystalline, with a grain size that is of the order of 25 nm. The figure also reveals clear lattice fringes within the grains, indicating that the oxide is crystalline and of high quality. The SADP and the integrated intensity profile in Fig. 2(b) show that, in agreement with the XRD pattern, the oxide phase is magnetite, Fe<sub>3</sub>O<sub>4</sub>. The hysteresis curves of a single-layer Fe<sub>3</sub>O<sub>4</sub> before and after annealing are shown in Fig. 3. Before annealing, the two distinctively different switching in the measured M–H loop indicated that there exist two magnetic phases, a soft phase and a hard phase, that are weakly coupled. This is consistent with the microscopic observations that Fe and Fe<sub>3</sub>O<sub>4</sub> phases are separated by a layer of paramagnetic FeO phase. After annealing at 150 °C for 5 h, the two-phase behavior of the film has given way to magnetically single-phase behavior, as seen in Fig. 3(b). The structure of the interface and the identity of the phases present in the magnetite layer in a layered stack are shown in Fig. 4. To analyze the phase, we have measured the d-spacings from the fast Fourier transformation (FFT) of high resolution image, which were used to determine the phase. Three phases are found at the interface in the unannealed sample, namely Fe, FeO, and Fe<sub>3</sub>O<sub>4</sub>. The Fe phase arises from the unstable plasma conditions at the start of the magnetite deposition, and the FeO phase appears to surround the soft Fe [Fig. 4(b)]. In our work, the FeO phase that surrounds the Fe before annealing is transformed into Fe and Fe<sub>3</sub>O<sub>4</sub> with annealing, which is consistent with previous work [11]. It should be noted that equilibrium FeO can be obtained only

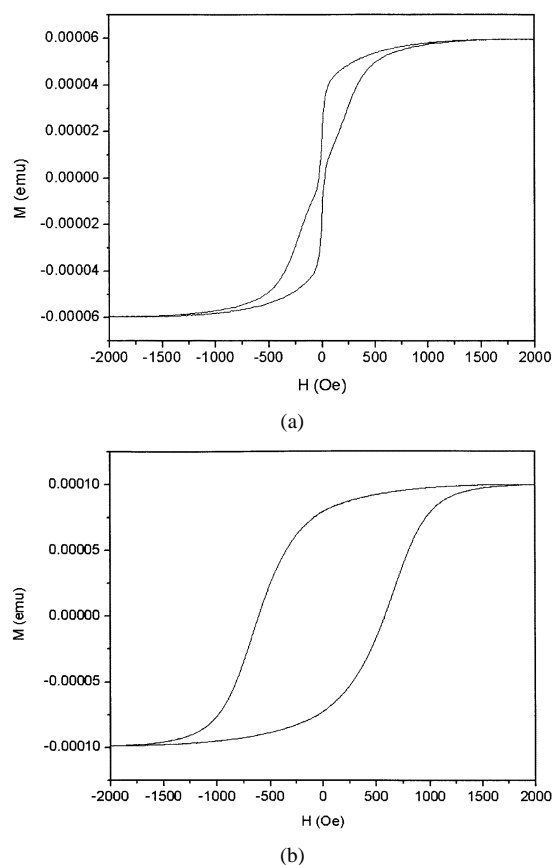


Fig. 3. M–H loops of Fe<sub>3</sub>O<sub>4</sub> 70-nm-thick film (a) before annealing and (b) after annealing.

above 570 °C [12]. Therefore, at the low annealing temperature used here, this metastable FeO transforms into the stable Fe or Fe<sub>3</sub>O<sub>4</sub>.

Based on the TEM observations, the M–H loops of Fig. 3 are interpreted as follows. In Fig. 3(a), the low coercivity in the sharp region in the loop is associated with Fe since this is the softest magnetic phase among the phases seen in the samples. Furthermore, since the Néel temperature of FeO is 198 K [13], FeO is paramagnetic at room temperature and results in weak magnetic coupling between Fe and Fe<sub>3</sub>O<sub>4</sub>. By contrast, in Fig. 3(b), the disappearance of FeO upon annealing leads to strong coupling between Fe and Fe<sub>3</sub>O<sub>4</sub> and gives rise to the increase in coercivity. The magnetoresistance transfer curves of the MTJ before and after annealing are shown in Fig. 5. All measurements were made at room temperature. There are two switching fields, H<sub>C1</sub> and H<sub>C2</sub>, which correspond to the coercivity of soft (NiFe) and hard magnetic materials (Fe or Fe<sub>3</sub>O<sub>4</sub>), respectively. Before annealing, an MR ratio of 3.5% and H<sub>C2</sub> of 40 Oe are observed, which is the characteristic of the Fe phase. Since both Fe and FeO coexist at the junction, we believe that the measured MR is mainly due to Fe at lower fields. To clarify the source of the low switching field and low MR in the unannealed sample, we made a MTJ of Ta 3 nm/NiFe 10 nm/AlO<sub>x</sub> 2.5 nm/Fe 5 nm/Ta 3 nm. This junction has an MR ratio of 18% and H<sub>C2</sub> of 40 Oe (not shown). The reason for the low MR ratio in our Fe<sub>3</sub>O<sub>4</sub> junction is the presence of FeO phase at the interface, which is confirmed by HRTEM. Even though an Fe electrode itself can produce a relatively high MR ratio, the presence of the

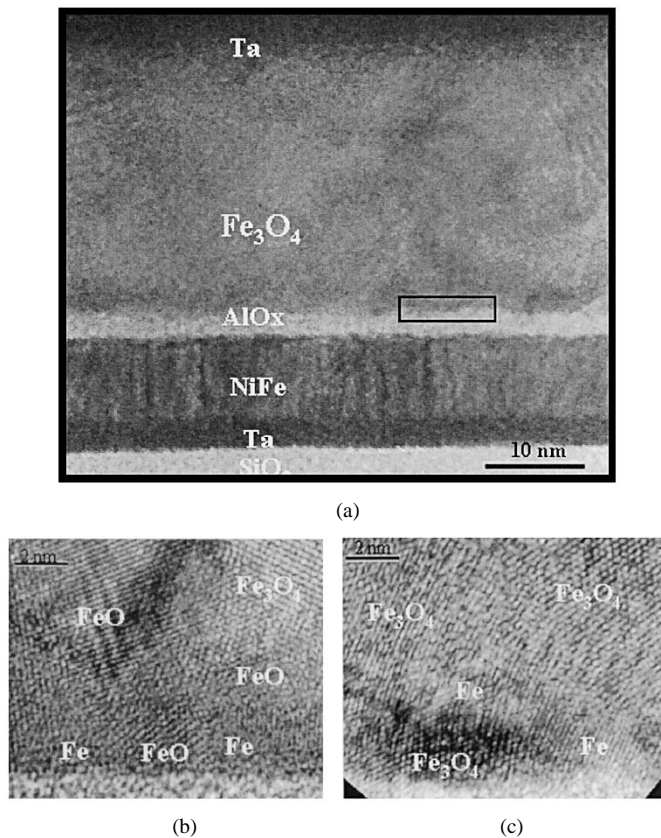


Fig. 4. Cross-sectional transmission electron micrographs of Ta 5 nm/NiFe 10 nm/ $\text{AlO}_x$  2.5 nm/ $\text{Fe}_3\text{O}_4$  30 nm/Ta 5 nm film stacks, (a) and (b) as-deposited, and (c) annealed at 150 °C for 5 h; Fig. (a) is a low magnification image, while (b) and (c) are high resolution images. The inset box indicates the position at which the high resolution image is taken.

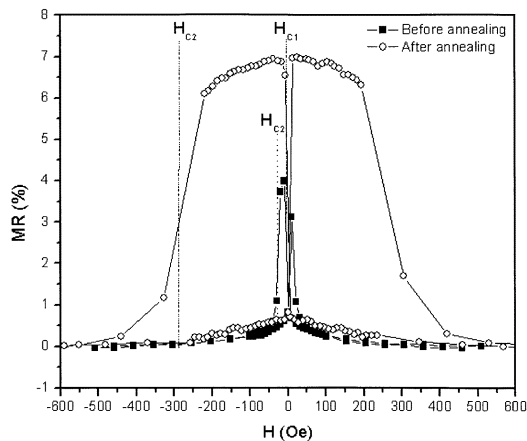


Fig. 5. Magnetoresistance transfer curve of junction structure (Ta 5 nm/NiFe 10 nm/ $\text{AlO}_x$  2.5 nm/ $\text{Fe}_3\text{O}_4$  30 nm/Ta 5 nm) before and after annealing.

paramagnetic FeO produces a low MR ratio. After annealing, the MR as well as the  $H_{C2}$  increases more than a factor of two, resulting in the increased MR (7.0%) and higher switching field

( $H_{C2}$ ) (300 Oe). However, annealing does not remove all the Fe at the interface, which prevents us from realizing the full potential of  $\text{Fe}_3\text{O}_4$ .

#### IV. CONCLUSION

Crystalline  $\text{Fe}_3\text{O}_4$  films have been fabricated by reactive sputtering, and the interface of a MTJ in a layered structure of oxidized silicon/Ta 5 nm/NiFe 10 nm/ $\text{AlO}_x$  2.5 nm/ $\text{Fe}_3\text{O}_4$  30 nm/Ta 5 nm has been studied. Three phases, namely, Fe, FeO, and  $\text{Fe}_3\text{O}_4$  phases, are found to coexist at the interface. Before annealing, the FeO magnetically decouples the Fe and  $\text{Fe}_3\text{O}_4$  phases. Before annealing, the junction has a MR ratio of 3.5% and  $H_{C2}$  of 40 Oe. Upon annealing, the FeO phase is transformed into the Fe and  $\text{Fe}_3\text{O}_4$ , leading to a strong coupling between the Fe and  $\text{Fe}_3\text{O}_4$ . Annealing also results in a relatively high MR ratio of 7.0% and higher  $H_{C2}$  of 300 Oe. It is concluded that the presence of FeO and Fe at the interface of  $\text{Fe}_3\text{O}_4$  with an  $\text{AlO}_x$  tunneling barrier destroys the spin polarization of the tunneling electrons, thereby limiting the MR to a relatively low value. However, modification of the plasma conditions at the start of magnetite deposition is expected to lead to purely single phase  $\text{Fe}_3\text{O}_4$  with high spin polarization.

#### REFERENCES

- [1] Z. Zhang and S. Satpathy, "Electron states, magnetism, and the Verwey transition in magnetite," *Phys. Rev.*, vol. 44, pp. 13 319–13 331, 1991.
- [2] J. M. D. Coey and M. Venkatesan, "Half-metallic ferromagnetism: Example of  $\text{CrO}_2$ ," *J. Appl. Phys.*, vol. 91, pp. 8345–8350, 2002.
- [3] K. Ghosh, S. B. Ogale, S. P. Pai, M. Robson, E. Li, I. Jin, Z.-W. Dong, R. L. Greene, R. Ramesh, T. Venkatesan, and M. Johnson, "Positive giant magnetoresistance in a  $\text{Fe}_3\text{O}_4/\text{SrTiO}_3/\text{La}_{0.7}\text{Sr}_{0.3}\text{MnO}_3$  heterostructure," *Appl. Phys. Lett.*, vol. 73, pp. 689–691, 1998.
- [4] P. Sensor, A. Fert, J.-L. Maurice, F. Montaigne, F. Petroff, and A. Vaures, "Large magnetoresistance in tunnel junctions with an iron oxide electrode," *Appl. Phys. Lett.*, vol. 74, pp. 4017–4019, 1999.
- [5] X. Li, A. Gupta, G. Xiao, W. Qian, and P. David, "Fabrication and properties of heteroepitaxial magnetite ( $\text{Fe}_3\text{O}_4$ ) tunnel junctions," *Appl. Phys. Lett.*, vol. 73, pp. 3282–3284, 1998.
- [6] K.-I. Aoshima and S. X. Wang, " $\text{Fe}_3\text{O}_4$  and its magnetic tunneling junctions grown by ion beam deposition," *J. Appl. Phys.*, to be published.
- [7] G. Hu and Y. Suzuki, "Negative spin polarization of  $\text{Fe}_3\text{O}_4$  in magnetite/manganite-based junctions," *Phys. Rev. Lett.*, vol. 89, pp. 276 601/1–4, 2002.
- [8] P. Shah, M. Sohma, K. Kawaguchi, and I. Yamaguchi, "Growth conditions, structural and magnetic properties of  $\text{M}/\text{Fe}_3\text{O}_4/\text{I}$  ( $\text{M} = \text{Al}, \text{Ag}$  and  $\text{I} = \text{Al}_2\text{O}_3, \text{MgO}$ ) multilayers," *J. Magn. Magn. Mater.*, to be published.
- [9] S. S. P. Parkin, R. Sigsbee, R. Felici, and G. P. Felcher, "Observation of magnetic dead layers at the surface of iron oxide films," *Appl. Phys. Lett.*, vol. 48, pp. 604–606, 1986.
- [10] J. L. Labar, "ProcessDiffraction: A computer program to process electron diffraction patterns from polycrystalline or amorphous films," in *Proc. EUREM 12*, vol. III, L. Frank and F. Ciampor, Eds., Brno, 2000, pp. I379–380.
- [11] T. S. Chin and N. C. Chiang, "Magnetic properties of sputtered  $\text{Fe}_{1-x}\text{O}$  and  $\text{Fe} + \text{Fe}_3\text{O}_4$  thin films," *J. Appl. Phys.*, vol. 81, pp. 5250–5252, 1997.
- [12] T. B. Massalski, *Binary Alloy Phase Diagrams*. Materials Park, OH: ASM Int., 1990, vol. 2, pp. 1739–1744.
- [13] M. S. Seehra and G. Srinivasan, "Magnetic studies of nonstoichiometric  $\text{Fe}_2\text{O}$  and evidence for magnetic defect clusters," *J. Phys. C, Solid State Phys.*, vol. 17, pp. 883–892, 1984.